

# Real-Time Monitoring of Yeast Cell Division by Dielectric Spectroscopy

K. Asami,\* E. Gheorghiu,# and T. Yonezawa§

\*Institute for Chemical Research, Kyoto University, Uji, Kyoto 611-0011, Japan; #National Institute of Biotechnology, UNESCO Center of Biodynamics, 77102 Bucharest 1, Romania; and §Production Division I, Suntory, Osaka 618-0001, Japan

**ABSTRACT** To assay cell cycle progression in synchronized culture of yeast we have applied dielectric spectroscopy to its real-time monitoring. The dielectric monitoring is based on the electromagnetic induction method, regarded as a nonelectrode method, which has resolved the problems encountered in measurements with metal electrodes, namely electrode polarization and bubble formation on electrodes. In the synchronized culture with temperature-sensitive cell division cycle mutants, the permittivity of the culture broth showed cyclic changes at frequencies below 300 kHz. The increase and decrease in the cyclic changes of the relative permittivity correspond to the increase in cell length and bud size and to the septum formation between mother and daughter cells, respectively.

## INTRODUCTION

Synchronized cell culture is an indispensable technique in cell cycle research. To assay synchronous cell growth, cells are sampled at a regular interval over a few cell cycles, and the changes in morphology and DNA content are examined by optical microscopy and flow cytometry (Hass and Lew, 1997), respectively. Unfortunately, the examinations are time-consuming and laborious tasks, and therefore alternative methods capable of real-time and in situ measurement become increasingly important for precise analysis of cell cycle progression and for screening mutants. Dielectric spectroscopy can be a most suitable method for this purpose because of the noninvasive and rapid measurement sensitive to the morphological and electrical properties of cells.

Biological cells are polarized in an ac field owing to interfacial polarization that is the accumulation of charges at the boundaries between the membrane and aqueous phases of different electrical properties (Schwan, 1957; Pethig, 1979; Takashima, 1989; Asami, 1998). The interfacial polarization depends on frequency of the applied ac field and shows relaxation. Since a cell is covered with a thin and insulating membrane, the polarization becomes huge at low frequencies, and the corresponding equivalent, homogeneous relative permittivity ( $\epsilon_c$ ) of the cell is on the order of 1000. For the cell suspension, therefore, the increment  $\delta\epsilon$  in relative permittivity (or the difference in relative permittivity between the cell suspension and the suspending medium) is proportional to the content of cells, thereby allowing the estimation of biomass by dielectric measurement (Harris et al., 1987; Mishima et al., 1991). The  $\delta\epsilon$  also shows frequency dependence, namely dielectric dispersion or relaxation, of which magnitude and characteristic frequency are a function of the morphological and electrical parameters of

cells. Therefore, monitoring the dielectric dispersion would enable us to follow the cell cycle progression.

Despite the potential benefits of dielectric spectroscopy, however, it has not been used for the real-time monitoring of synchronous cell growth because of three technical problems encountered in the measurements. First, the most serious problem that comes from culture media containing electrolytes is electrode polarization due to the electrical double layer between metal electrodes and an electrolyte solution (Schwan, 1963). The large capacitive component of the electrical double layer masks the small change in relative permittivity produced by cell growth, whose value is at most a few tens. Second, it is still difficult to precisely determine such a small permittivity component from the almost entirely conductive admittance, even if the problem of electrode polarization could be solved. Third, CO<sub>2</sub> generated in fermentation forms bubbles on metal electrode surfaces, which interfere with the measurements. These problems are not necessarily serious in the case of the real-time estimation of biomass, and the conventional electrode methods are applicable to it (Harris et al., 1987; Asami and Yonezawa, 1995a). However, the monitoring of the cell cycle progression in synchronized culture requires greater precision and stability in measurement than the biomass estimation, so that it is essential to overcome the problems.

The difficult requirements for the measurement have been resolved by a new method developed by Wakamatsu (1997). This method, based on electromagnetic induction, is termed the electromagnetic induction method and is regarded as a nonelectrode method. In this paper we demonstrate that synchronous yeast growth can be monitored by dielectric spectroscopy coupled with the electromagnetic induction method.

## MATERIALS AND METHODS

### Dielectric measurement

The electromagnetic induction method uses an epoxy resin-coated inductive probe consisting of two concentric toroidal coils that are inductively coupled through the admittance of the surrounding sample liquid (Fig. 1).

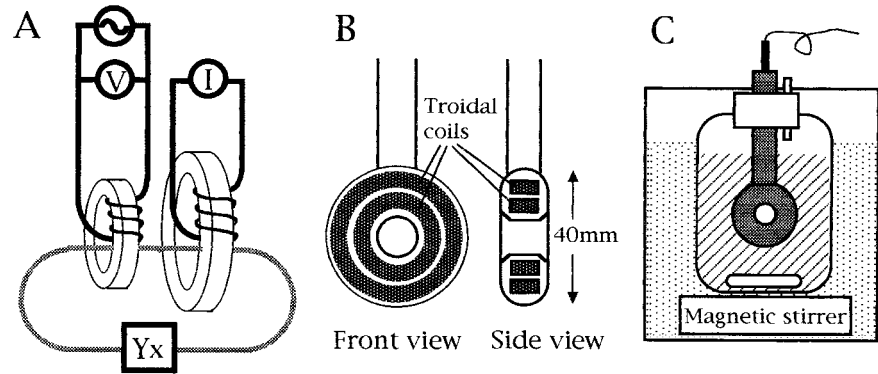
Received for publication 2 November 1998 and in final form 6 March 1999.

Address reprint requests to K. Asami, Institute for Chemical Research, Kyoto University, Uji, Kyoto 611-0011, Japan. Tel.: 81-774-32-3111 ext. 2080; Fax: 81-774-38-3084; E-mail: [asami@tampopo.kuicr.kyoto-u.ac.jp](mailto:asami@tampopo.kuicr.kyoto-u.ac.jp).

© 1999 by the Biophysical Society

0006-3495/99/06/3345/04 \$2.00

FIGURE 1 (A) The principle of the electromagnetic induction method. When an ac voltage  $V$  is applied to the primary troidal coil, an electric field is induced in the sample of the admittance  $Y_x$  surrounding the probe, thereby an electric current  $I$  takes place in the secondary troidal coil. The comparison of  $I$  with  $V$  provides  $Y_x$ , from which the relative permittivity and conductivity of the sample are determined. (B) The inductive probe used for the electromagnetic induction method. (C) The probe mounted in the culture system with a water bath.



The applied voltage to the primary troidal coil and the output current from the secondary one are compared using a 4285A Precision LCR Meter (Hewlett-Packard Co., Palo Alto, CA) to determine the relative permittivity and conductivity of the sample over a frequency range of 75 kHz to 30 MHz. The inductive probe used was the same as that described in a previous paper (Wakamatsu, 1997).

To improve the accuracy of the measurement, the measurement system was calibrated using special 0-ohm and 50-ohm standards, and correction was made for the residual admittance of the probe, as described by Wakamatsu (1997).

The probe was mounted in a 500-ml bottle containing 400 ml culture broth. The bottle was placed in a water bath, whose temperature was regulated within  $\pm 0.03^\circ\text{C}$  with a CTE42A Coolnics Circulator (Yamato-Komatsu, Tokyo). The culture broth was stirred with a magnetic stirrer. The noise level and stability in the measurement were tested with a culture medium whose conductivity was  $0.37 \text{ Sm}^{-1}$  at  $25^\circ\text{C}$ . The fluctuation in relative permittivity was within 0.1–0.2 between 100 kHz and 200 kHz and  $<0.1$  between 200 kHz and 30 MHz. The excellent stability and low noise level of the permittivity measurement allowed us to monitor the cell cycle progression in synchronized culture.

## Synchronized culture

For synchronized cell culture, temperature-sensitive cell-division-cycle (*cdc*) mutants of budding and fission yeast were used. The *cdc* 28-13 (SH3009) of *Saccharomyces cerevisiae* arrests predominantly at “Start,” and the *cdc* 25-22 (K164-9) of *Schizosaccharomyces pombe* cannot enter mitosis, at a restrictive temperature of  $36^\circ\text{C}$  (Murray and Hunt, 1993). The cells were inoculated at 2.5–10% of the final cell concentration in 400 ml YEPD medium containing 2% glucose, 2% polypeptone, and 1% yeast extract, and were precultured at  $36^\circ\text{C}$  for 2 h (SH3009) and for 4 h (K164-9) to obtain the arrested cells. The synchronous growth of the cells was started by lowering the temperature to a permissive temperature of  $25^\circ\text{C}$ .

## Morphology

The micrographs of the cells sampled at a regular interval from the culture broth were obtained using a phase contrast microscope with a CCD video camera. The image analysis of the micrographs was carried out using Image-Pro (Media Cybernetics, Silver Spring, MD).

## RESULTS AND DISCUSSION

Figs. 2 and 3 show the time course of the  $\delta\epsilon$  in the synchronous and asynchronous growth of SH3009 and K164-9 cells. The cells were inoculated at 5% of the final cell concentration, so that at most four cell cycles should have

been expected. For the synchronized culture of SH3009 cells, the  $\delta\epsilon$  at low frequencies (0.17 and 0.37 MHz) showed oscillation, while at high frequencies (above 0.82 MHz), the  $\delta\epsilon$  increased monotonously up to 12 h in the same manner as in the asynchronous growth. In the oscillation, four cycles were clearly distinguishable and the time per one cycle was  $\sim 100$  min except for the last cycle. The number of the permittivity cycles was closely related to the concentration of inoculated cells, e.g., five and three cycles were found for 2.5% and 10% of the final cell concentration, respectively.

In the synchronized culture of K164-9 cells, the time course of the  $\delta\epsilon$  has characteristics essentially similar to those for SH3009 cells, i.e., the effect of synchronization appears only at low frequencies but does not at high frequencies. However, some differences are also seen between the two strains. K164-9 cells showed only one and one-half

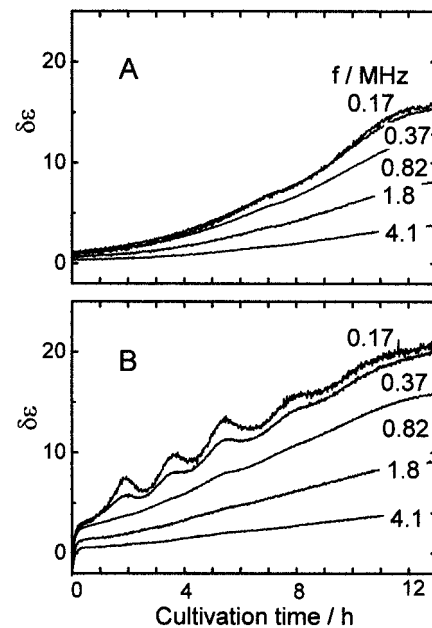


FIGURE 2 The relative permittivity change  $\delta\epsilon$  of the culture broth in the asynchronous (A) and synchronous (B) growth of *cdc* 28-13 (SH3009) of *S. cerevisiae*.

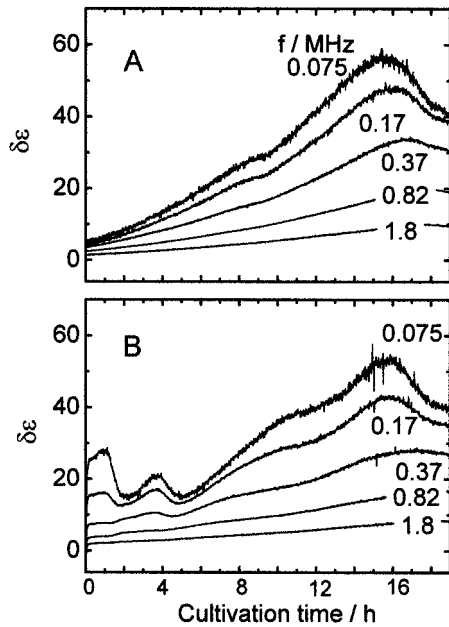


FIGURE 3 The relative permittivity change  $\Delta\epsilon$  of the culture broth in the asynchronous (A) and synchronous (B) growth of *cdc 25-22* (K164-9) of *S. pombe*.

cycles, which began after a time lag of  $\sim 1$  h as though the oscillation was out of phase by  $180^\circ$  with that for SH3009. The number of the permittivity cycles was independent of the concentration of inoculated cells, in contrast to SH3009 cells.

To correlate the cyclic changes in relative permittivity to the cell division cycle, the morphology of cells was examined simultaneously with dielectric monitoring. Fig. 4 shows a typical set of results with K164-9 cells, whose septum formation can be clearly detected by phase contrast microscopy (see Fig. 5 B, inset). After the lag phase of  $\sim 60$  min the septation index or the percentage of cells with septa increased to reach a maximum at  $\sim 120$  min (Fig. 4 B). The increase in the septation index in this period was fully correlated with the decrease in the low-frequency  $\Delta\epsilon$  in Fig. 4 A. The successive apparent cell separation in the period from 120 min to 180 min, which appeared as the decreases in the septation index and in the mean cell length/diameter ratio, caused a relatively small change in  $\Delta\epsilon$ . In the second cycle starting from  $\sim 180$  min, the low-frequency  $\Delta\epsilon$  increased with the cell elongation and then decreased. However, the decrease in  $\Delta\epsilon$  no longer coincided in time with the increase in the septation index because of the low synchrony in the second cell division cycle.

Fig. 5 shows frequency dependence of the  $\Delta\epsilon$  obtained at points 1 and 2 in Fig. 4 A, where most cell populations lack and possess septa, respectively (see micrographs in Fig. 5, A and B, insets). The dielectric dispersions were represented by a sum of two subdispersions of the Cole-Cole type (Cole and Cole, 1941). The low-frequency subdispersion was very sensitive to the septum formation; the amplitude decreases by  $\sim 50\%$  and the characteristic frequency was approxi-

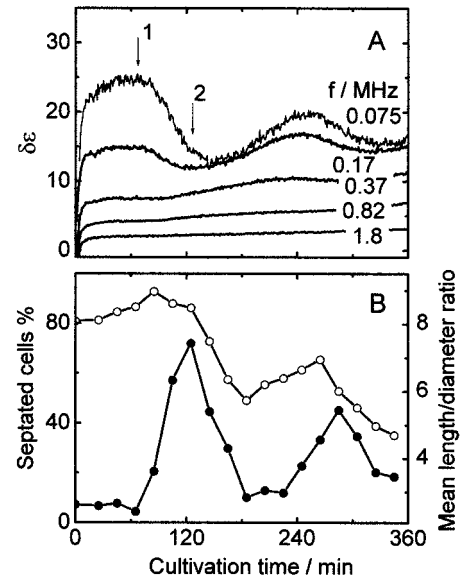


FIGURE 4 Comparison between the dielectric and morphological properties in the synchronous growth of *cdc 25-22* (*S. pombe*). (A) The relative permittivity change  $\Delta\epsilon$  of the culture broth. (B) The septation index (filled circles) and the mean length/diameter ratio (open circles). Most cell populations lack and possess septa at the points 1 and 2, respectively.

mately doubled by the onset of septation. In contrast, the high-frequency subdispersion was little influenced by the septum formation. According to the dielectric theory based

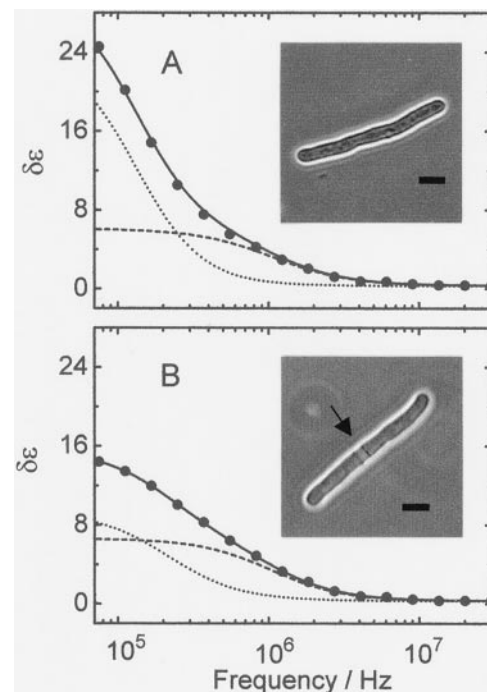


FIGURE 5 Frequency dependence of  $\Delta\epsilon$  obtained at points 1 (A) and 2 (B) indicated in Fig. 4 A, which is decomposed into two subdispersions of the Cole-Cole type, which are indicated by the broken and dotted lines. Insets: phase-contrast micrographs of the representative cells. The arrow in B indicates the septum. Scale bar, 10  $\mu\text{m}$ .

on an ellipsoidal cell model (Asami and Yonezawa, 1995b), the high- and low-frequency subdispersions are respectively attributed to the radial and longitudinal components ( $\epsilon_{cr}$  and  $\epsilon_{cl}$ ) of the equivalent, homogeneous relative permittivities  $\epsilon_c$  of a cell. The longitudinal component  $\epsilon_{cl}$  is determined when an electric field is applied to the cell in its longitudinal direction, so that the electric field crosses the septum. This is the reason why the  $\epsilon_{cl}$  is much more sensitive to the septum formation than the  $\epsilon_{cr}$ .

In Fig. 6 we attempt to give an intuitive explanation for the effect of the septum formation on the  $\epsilon_{cl}$  using a simple equivalent circuit model. A cylindrical cell of length  $l$  and circular area  $S$  as a model of fission yeast is placed between two disk electrodes such that the electric field is parallel to the longitudinal direction. The equivalent circuit for the cell without septum may be represented by a series combination of two capacitors of  $C$  ( $C = SC_m$ , where  $C_m$  is the specific membrane capacitance of the plasma membrane) and a resistor of  $R$  for the cytoplasm, while for the septated cell, two more capacitors due to the septum are added in series. Hence, the  $\epsilon_{cl}$  shows relaxation with the time constant of  $RC/2$  for the cell without septum and  $RC/4$  for the septated cell if the same cytoplasmic resistance is shared by both models. The low-frequency limit of the  $\epsilon_{cl}$  for the cell without septum is given by  $\epsilon_{cl} = IC_m/2\epsilon_0$ , where  $\epsilon_0$  is the permittivity of vacuum, being proportional to the cell length and becoming 50% by the onset of septation, i.e.,  $\epsilon_{cl} = IC_m/4\epsilon_0$ . This provides a qualitative explanation of the experimentally observed changes in the low-frequency subdispersion in the septation and cell elongation. A similar explanation is also applicable to budding yeast (SH3009), i.e., the increase in  $\delta\epsilon$  at low frequencies corresponds to the increase in bud size and the decrease to the formation of septum between mother cell and bud (Asami et al., 1998).

The quantitative analysis of the electrical properties of cells in cell division is an important issue, but the awkward

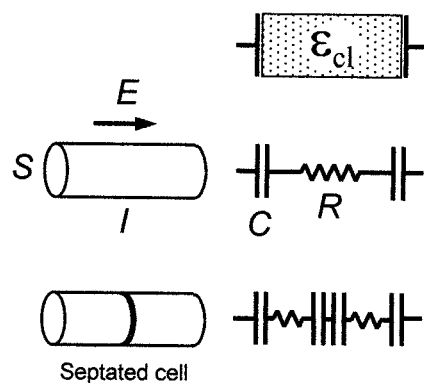


FIGURE 6 An intuitive explanation for the changes in the longitudinal component  $\epsilon_{cl}$  of the homogeneous, equivalent relative permittivity of a cylindrical cell by the septum formation. In the equivalent electrical circuits, the capacitors of  $C$  due to the plasma membranes perpendicular to an electric field  $E$  and the resistor of  $R$  due to the cytoplasm are combined in series.

and complicated morphology of budding and septated cells is an obstacle to it because their polarization in an electric field cannot be solved analytically. In previous papers we assumed simple electrical cell models and simulated the cyclic changes in relative permittivity in synchronized culture (Asami and Yonezawa, 1995b; Gheorghiu and Asami, 1998). Although the simulations provide dielectric behavior very similar to that obtained in the present study, the simplified models cannot be used for properly estimating the electrical parameters of cells from the observed dielectric dispersion. Therefore, we are now developing a sophisticated method for the numerical calculation with more realistic cell models.

We thank Dr. S. Harashima (Osaka University) for the gift of SH3009 strain, and Dr. K. Tamai and Dr. C. Shimoda (Osaka City University) for the gift of K164-9 strain. We also thank H. Wakamatsu and N. Koyanagi (Japan Hewlett-Packard) for their advice on the electromagnetic induction method and Dr. A. Irimajiri (Kochi Medical School) for critical reading of this manuscript.

This work was supported by Ministry of Education, Culture and Science, Japan (Grant 09555252).

## REFERENCES

- Asami, K. 1998. Dielectric relaxation spectroscopy of biological cell suspensions. *In Handbook on Ultrasonic and Dielectric Characterization Techniques for Suspended Particulates*. V. A. Hackley and J. Texter, editors. The American Ceramic Society, Westerville, OH. 333–349.
- Asami, K., E. Gheorghiu, and T. Yonezawa. 1998. Dielectric behavior of budding yeast in cell separation. *Biochim. Biophys. Acta*. 1381:234–240.
- Asami, K., and T. Yonezawa. 1995a. Dielectric analysis of yeast cell growth. *Biochim. Biophys. Acta*. 1245:99–105.
- Asami, K., and T. Yonezawa. 1995b. Dielectric behavior of nonspherical cells in culture. *Biochim. Biophys. Acta*. 1245:317–324.
- Cole, K. S., and R. H. Cole. 1941. Dispersion and absorption in dielectrics. I. Alternating current characteristics. *J. Chem. Phys.* 9:341–351.
- Gheorghiu, E., and K. Asami. 1998. Monitoring cell cycle by impedance spectroscopy: experimental and theoretical aspects. *Bioelectrochem. Bioenerg.* 45:139–143.
- Harris, C. M., R. W. Todd, S. J. Bungard, R. W. Lovitt, G. Morris, and D. B. Kell. 1987. Dielectric permittivity of microbial suspensions at radio frequencies: a novel method for the real-time estimation of microbial biomass. *Enzyme Microb. Technol.* 9:181–186.
- Hass, S. B., and D. J. Lew. 1997. Flow cytometric analysis of DNA content in budding yeast. *In Methods in Enzymology*, Vol. 283: Cell Cycle Control. W. G. Dunphy, editor. Academic Press, New York. 322–332.
- Mishima, K., A. Mimura, Y. Takahara, K. Asami, and T. Hanai. 1991. On-line monitoring of cell concentrations by dielectric measurements. *J. Ferment. Bioeng.* 72:291–295.
- Murray, A., and T. Hunt. 1993. *The Cell Cycle*. Oxford University Press, New York and Oxford.
- Pethig, R. 1979. *Dielectric and Electronic Properties of Biological Materials*. John Wiley and Sons, New York.
- Schwan, H. P. 1957. Electrical properties of tissue and cell suspensions. *In Advances in Biological and Medical Physics*, Vol. 5. J. H. Lawrence and C. A. Tobias, editors. Academic Press, New York. 147–209.
- Schwan, H. P. 1963. Determination of biological impedance. *In Physical Techniques in Biological Research*, Vol. 6. W. L. Nastuk, editor. Academic Press, New York and London. 323–406.
- Takashima, S. 1989. *Electrical Properties of Biopolymers and Membranes*. Adam Hilger, Bristol, UK.
- Wakamatsu, H. 1997. A dielectric spectrometer for liquid using the electromagnetic induction method. *Hewlett-Packard J.* 48:37–44.